Ionics (2017) 23:2367–2376
DOI 10.1007/s11581-017-2088-8

ORIGINAL PAPER

Fuel cell and electrochemical studies of the ethanol electro-oxidation in alkaline media using PtAuIr/C as anodes

Sirlane G. da Silva [1] · Eric H. Fontes [1] · Mônica H.M.T. Assumpção [2] · Marcelo Linardi [1] · Estevam Spinacé [1] · Júlio César M. Silva [1] · Almir O. Neto [1]

Received: 19 December 2016 / Revised: 10 March 2017 / Accepted: 27 March 2017 / Published online: 11 April 2017

Abstract Ethanol electro-oxidation reaction was investigated considering conventional electrochemical experiments in alkaline media, direct ethanol fuel cell (DEFC), and in situ ATR-FTIR. The working electrode/anodes were composed of monometallic Pt/C, Au/C, Ir/C, and trimetallic PtAuIr/C nanoparticles with atomic Pt/Au/Ir ratios of 40:50:10, 50:40:10, 60:30:10, 70:20:10, and 80:10:10. X-ray diffraction (XRD) suggests PtAuIr/C alloy formation, and according to transmission electron micrographs, the mean particle sizes are from 4 to 6 nm for all catalyst compositions. PtAuIr/C 40:50:10 showed the highest catalytic activity for ethanol electro-oxidation in the electrochemical experiments; using this material, the peak current density from ethanol electro-oxidation on cyclic voltammetry experiment was 50 mA per g of Pt, 3.5 times higher than that observed with Pt/C. The fuel cell performance was superior using all PtAuIr/C compositions than using Pt/C. Au/C and Ir/C presented very poor catalytic activity toward ethanol electro-oxidation. The improved results obtained using PtAuIr/C might be related to the OH_{ads} species formed at low overpotential on Ir and to the decrease on adsorption energy of poisoning intermediates on Pt sites, promoted by Au.

Keywords PtAuIr/C electrocatalysts · Ethanol electro-oxidation · DEFC

✉ Almir O. Neto
aolivei@ipen.br

[1] Instituto de Pesquisas Energéticas e Nucleares, IPEN/CNEN-SP, Av. Prof. Lineu Prestes, 2242 Cidade Universitária, São Paulo, SP 05508-900, Brazil

[2] Universidade Federal de São Paulo, UFSCar, Campus Lagoa do Sino, Rodovia Lauri Simões de Barros, Km 12, Buri, SP 18290-000, Brazil

Introduction

The use of fossil fuels has resulted in an increase of CO_2 concentration in the atmosphere [1]. It is well known that CO_2 emission from fossil fuels is one of the principals responsible for the greenhouse effect. Taking these aspects into account, fuel cells might be an excellent alternative to the current energy generation as a clean and efficient power source [2]. In this context, alkaline fuel cells have attracted worldwide attention due to its promise to produce clean energy with high efficiency [2, 3].

Among different fuels, ethanol has been pointed out as an excellent alternative since it is carbon neutral, because it is produced from biomass, presents low toxicity, and has high energy density (8.0 kWh kg^{-1}) [4, 5]. Thus, direct ethanol fuel cell could offer an alternative for electrical energy generation. The complete oxidation of ethanol to CO_2 involves 12 electrons [6]. However, the complete oxidation of ethanol to CO_2 requires the C–C bond cleavage, which is difficult at low temperature [7, 8]. Therefore, acetaldehyde and acetic acid (acetate in alkaline media) are dominant products, which involve only two and four electrons, respectively [9, 10].

Considering ethanol electro-oxidation, Pt has been identified as one of the best electrocatalysts for this process. However, it suffers from deactivation by CO poisoning intermediate [3, 11, 12]. In order to increase the catalytic activity of Pt for ethanol electro-oxidation, different elements have been added to Pt-based materials [4, 13–18]. Taking into account the ethanol electro-oxidation in alkaline media, Au has been pointed out as a good option to be combined with Pt (PtAu) [3]. Au decreases the adsorption energy of the poisoning intermediates on Pt due to the upshift in the d-band energy of Pt which may enhance the dissociation of the reaction products from the catalyst surface [19]. PtAu alloy might also increase

the C–C bond cleavage due to the extending lattice parameters of Pt [3].

It is reported that iridium increases the platinum activity for ethanol electro-oxidation which is associated to the hydroxyl groups that are more easily formed on Ir at low potentials, which assist in the oxidation of adsorbed intermediates from ethanol electro-oxidation [4, 20, 21]. The incorporation of Ir to Pd, producing PdIr/C, improved the catalytic activity of Pd toward ethanol electro-oxidation in alkaline media [5]. Moreover, PtIr/C also shows higher catalytic activity for ethanol electro-oxidation in alkaline media than Pt/C [20].

Considering the efforts to enhance the catalytic activity of the materials for ethanol electro-oxidation, trimetallic electrocatalysts have been proposed [4, 22–24]. Dutta et al. [22] reported that trimetallic PtPdAu/C materials show higher catalytic activity toward ethanol electro-oxidation than bimetallic PtAu/C and PtPd/C, while Wang et al. [23] affirm that the addition of Pt to PdSn/C material improves the catalytic activity for ethanol electro-oxidation. As can be seen, the addition of a third metal may enhance the catalytic activity of the bimetallic material. However, an important aspect to be considered in the trimetallic materials is the molar ratio between the elements in the catalyst composition [4, 23].

Au and Ir improve the catalytic activity of the platinum-based materials for ethanol electro-oxidation; thus, in the present work, trimetallic PtAuIr/C electrocatalysts in different atomic rations were synthesized using sodium borohydride method and applied for ethanol electro-oxidation in alkaline medium. This work contemplates not only electrochemical studies but also fuel cell and ATR-FTIR experiments in order to obtain real conditions and also information about the products from ethanol electro-oxidation.

Experimental

PtAuIr/C electrocatalysts in different atomic ratios Pt/Au/Ir (80:10:10, 70:20:10, 60:30:10, 50:40:10, 40:50:10), Pt/C, Au/C, and Ir/C (20 wt.% of metal loading) were prepared by the sodium borohydride reduction process [3, 25] using $H_2PtCl_6{\cdot}6H_2O$ (Aldrich), $HAuCl_4{\cdot}3H_2O$ (Aldrich), and $IrCl_3{\cdot}H_2O$ (Sigma-Aldrich), as metal sources. In this process, Carbon Vulcan XC72 was firstly dispersed in an isopropyl alcohol/water solution (50/50, v/v). Then, the metal precursor was added and placed in an ultrasonic bath for 5 min. After that, a solution of $NaBH_4$ in 0.1 mol L^{-1} NaOH was added in one step under stirring at room temperature, and the resulting solution was then maintained under stirring for an additional 30 min. The final mixture was filtered and the solids washed with water and then dried at 70 °C for 2 h.

The electrocatalysts were characterized by X-ray diffraction (XRD) using a Rigaku diffractometer model MiniFlex II using Cu Kα radiation source (0.154 nm). The X-ray diffraction patterns were recorded in the 2θ range of 20° to 90° with a step size of 0.05° and an acquisition time of 2 s per step. Transmission electron microscopy (TEM) analysis has been carried out by a JEOL transmission electron microscope model JEM-2100 operated at 200 kV.

The electrochemical experiments were done by using a three-electrode conventional cell, using as reference electrode Ag/AgCl (KCl 3 mol L^{-1}) and Pt wire as a counter electrode. The work electrode was prepared using the thin porous coating technique as previously reported [3, 20]. The electrochemical experiments were done by cyclic voltammetry at a scan rate of 10 mV s^{-1} in 1 mol L^{-1} KOH in the presence and absence of 1 mol L^{-1} ethanol, while chronoamperometry was recorded in the same electrolyte containing 1 mol L^{-1} ethanol at −0.35 V for 30 min. All measurements were conducted at room temperature.

The fuel cell experiments were conducted using a single cell with 5 cm^2 of area. The temperature was set to 75 °C for the fuel cell and 85 °C for the oxygen humidifier. All the electrodes were constructed with 1 mg of Pt per square centimeter in the anode and in the cathode except for Au/C and Ir/C which contained 1 mg of Au or 1 mg of Ir per square centimeter. For all experiments, a commercial Pt/C (BASF) was used as cathode. Nafion® 117 membrane, previously exposed to 6 mol L^{-1} KOH for 24 h [26–29], was also used.

The spectro-electrochemical ATR-FTIR in situ measurements were performed by a Nicolet 6700 FT-IR spectrometer equipped with an MCT detector cooled with a liquid N_2, ATR accessory (PIKE® MIRacle with a diamond/ZnSe crystal plate); the experimental setup can be found in the literature [13, 30, 31].

The absorbance spectra were collected using the ratio R/R_0, where R represents a spectrum at a given potential and R_0 is the spectrum collected at −0.85 V. Positive and negative directional bands represent gain and loss of species at the

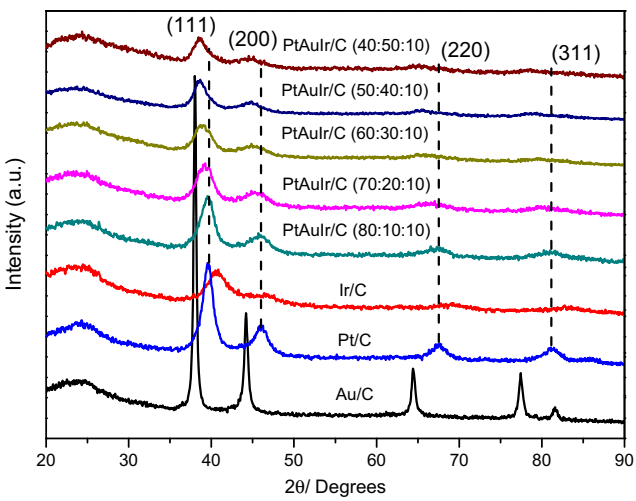

Fig. 1 X-ray diffraction patterns for the electrocatalysts

sampling potential, respectively. The spectra were computed from 128 interferograms averaged from 3000 to 850 cm^{-1} with the spectral resolution set to 8 cm^{-1}. Initially, a reference spectrum (R_0) was measured at −0.85 V, and the sample spectra were collected after applying successive potential steps from −0.85 to 0.05 V.

Results and discussion

X-ray diffraction patterns of the synthesized Pt/C, Au/C, Ir/C, and PtAuIr/C (40:50:10, 50:40:10, 60:30:10, 70:20:10, and 80:10:10) electrocatalysts are shown in Fig. 1. For all samples, it is possible to observe a broad peak of Vulcan Carbon

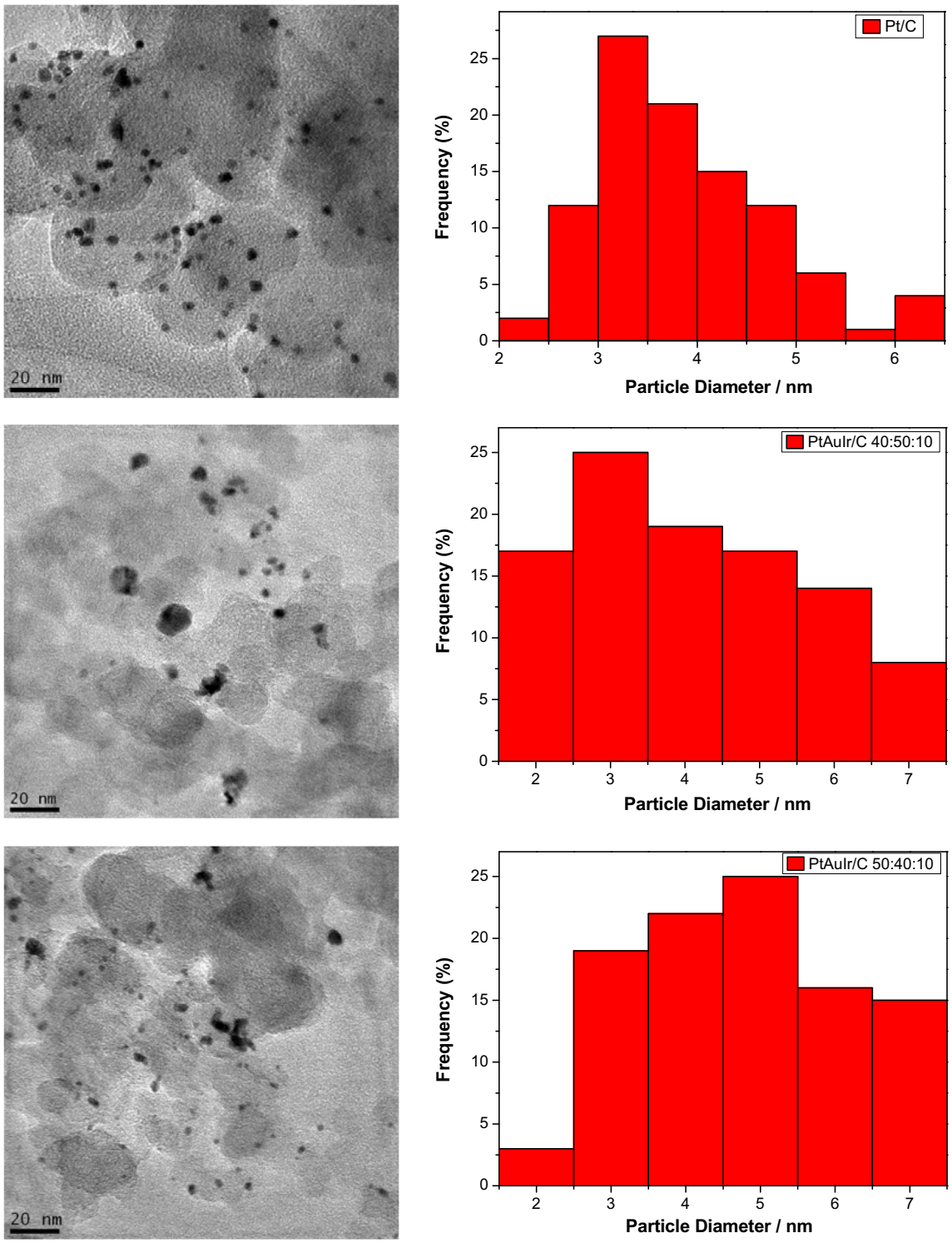

Fig. 2 TEM micrographs and histograms of the electrocatalysts prepared

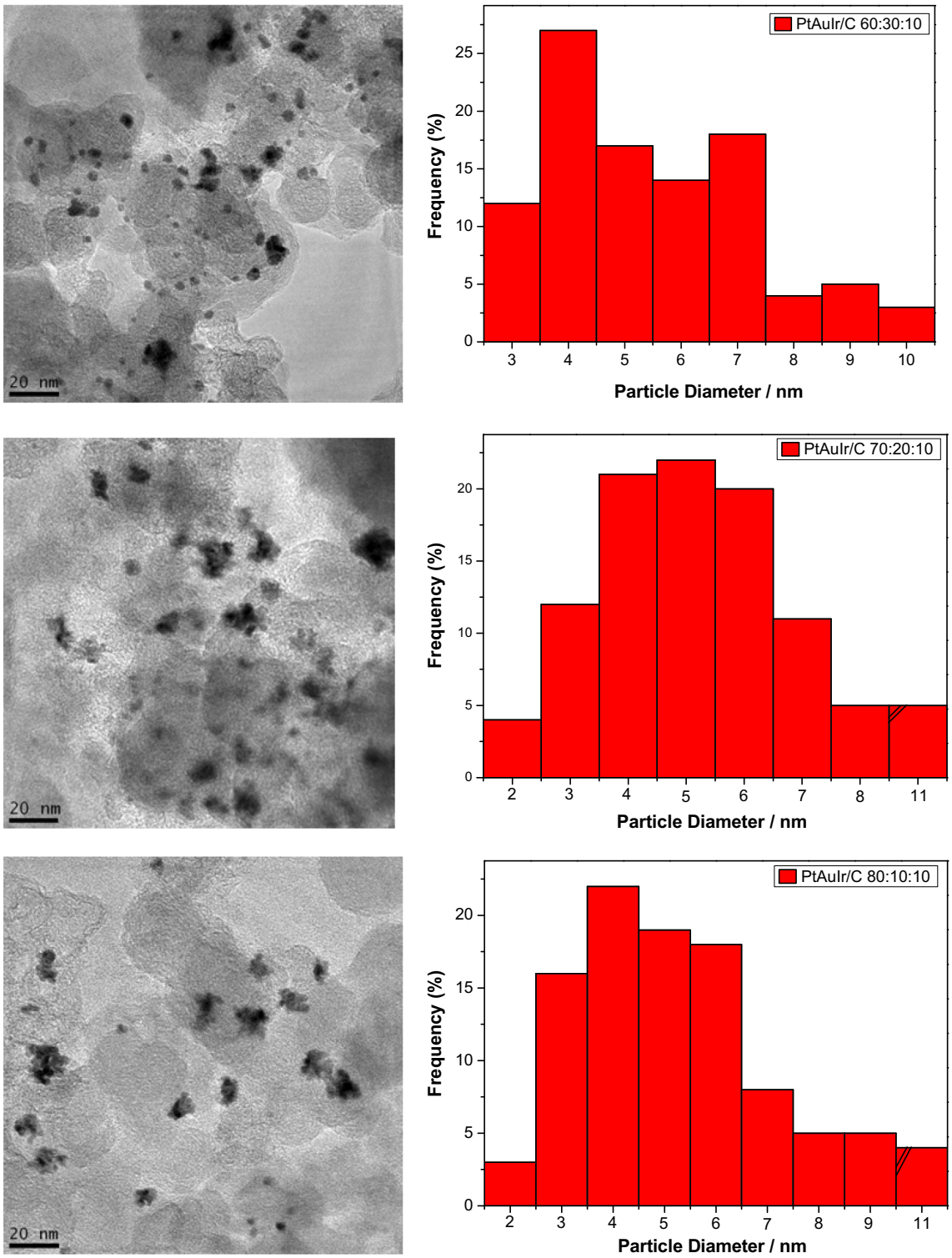

Fig. 2 continued.

centered at ~2θ of 25°, which correspond to the hexagonal structure of Vulcan carbon reflection (002) [3, 20]. The Au/C electrocatalyst shows the diffraction peaks at about 2θ = 38°, 45°, 65°, 78°, and 82°, attributed to the (111), (200), (220), (311), and (222) crystalline planes, respectively, indicating a typical face-centered cubic (fcc) crystalline structure of Au [32, 33]. The peaks at around 2θ = 39°, 46°, 67°, and 81° observed on the Pt/C patterns are attributed to the fcc structure of Pt that corresponds to (111), (200), (220), and (311) crystal planes, respectively [28, 34]. While the diffraction peaks at

around 2θ = 40°, 47°, 68°, and 82° on Ir/C are ascribed to Ir (111), (200), (220), and (311) crystalline planes, respectively, representing the characteristic diffraction of the fcc crystalline structure of Ir [35, 36]. For all PtAuIr/C patterns, it is possible to observe a shift in the position peaks to lower values at 2θ when compared to Pt/C, suggesting the formation of alloy [3, 37].

Figure 2 shows representative TEM micrographs and histograms of the particle mean diameter distribution for PtAuIr/C and Pt/C catalysts. In all cases, the particles were well dispersed on the carbon support. The mean diameters of the nanoparticles are 4.6 nm for PtAuIr/C 40:50:10, 5.3 nm for PtAuIr/C 50:40:10, 5.9 nm for PtAuIr/C 60:30:10, 5.7 nm for PtAuIr/C 70:20:10, 5.8 nm for PtAuIr/C 80:10:10, and 3.9 nm for Pt/C. The particle sizes agree to those synthesized by the sodium borohydride method in our recent publication [6, 20].

The cyclic voltammetry results in 1 mol L^{-1} KOH on Pt/C, Au/C, Ir/C, and PtAuIr/C electrocatalysts in the potential range from −0.85 to 0.05 V are shown in Fig. 3. The voltammogram of Pt/C displays a well-defined hydrogen oxidation region from −0.85 to −0.6 V [3, 20]. The region from −0.20 to 0.05 V is associated to the formation of an oxide layer on the platinum surface [38]. Ir/C and Au/C showed a similar shape to that previously reported in the literature [3, 20, 33, 35]. It is evident that as the Au content increases in the PtAuIr/C electrocatalysts, the voltammetric charge increases. This might be related to the large amount of gold oxides in the materials with higher amount of gold [3, 33]. In the PtAuIr/C materials, the two peaks related to the hydrogen adsorption/desorption process were suppressed due to the presence of gold and iridium; a similar comportment was also observed in the literature for PtAu/C and PtIr/C [3, 20].

Figure 4a shows the CVs of Pt/C, Au/C, Ir/C, and PtAuIr/C electrocatalysts in 1 mol L^{-1} KOH + 1 mol L^{-1} ethanol.

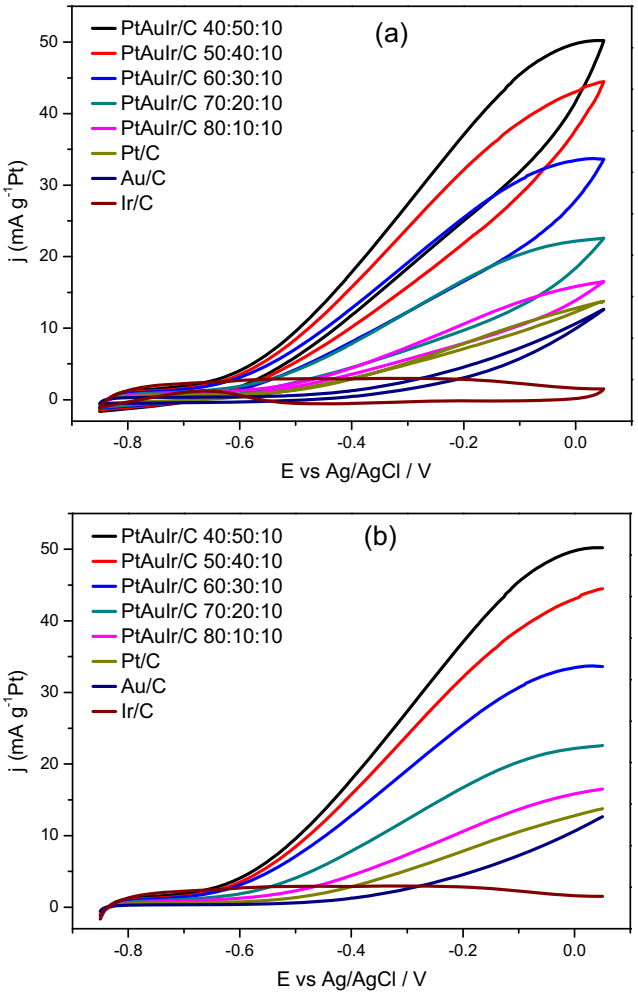

Fig. 4 Cyclic voltammograms for Pt/C, Ir/C, Au/C, and PtAuIr/C electrocatalysts in 1 mol L^{-1} KOH + 1 mol L^{-1} ethanol. Scan rate of 10 mV s^{-1} at room temperature

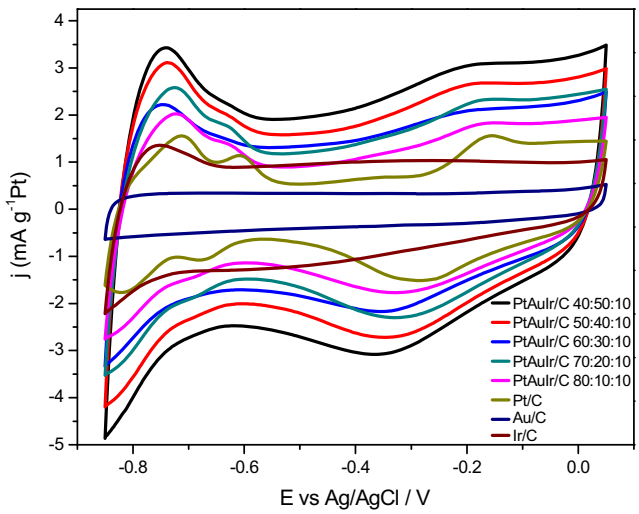

Fig. 3 Cyclic voltammograms for Pt/C, Ir/C, Au/C, and PtAuIr/C electrocatalysts in 1 mol L^{-1} KOH. Scan rate of 10 mV s^{-1} at room temperature

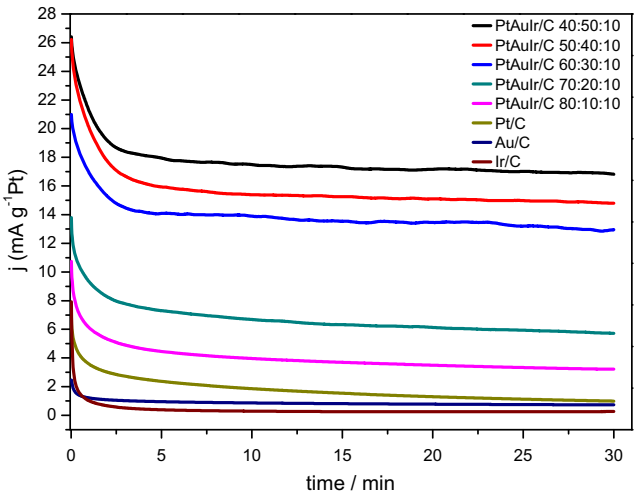

Fig. 5 Chronoamperometric measurements at −0.35 V for Pt/C, Ir/C, Au/C, and PtAuIr/C electrocatalysts in 1 mol L^{-1} KOH + 1 mol L^{-1} ethanol

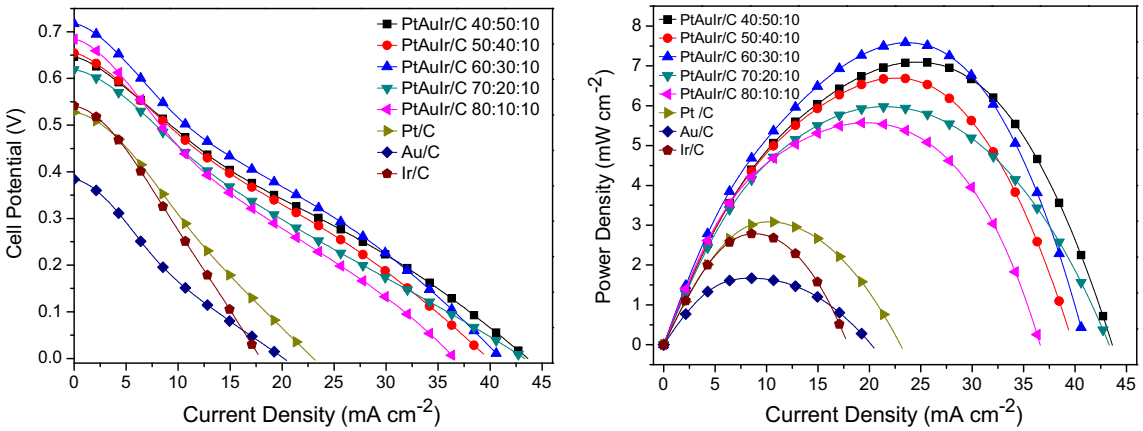

Fig. 6 Polarization and power density curves of a 5 cm^2 DEFC at 75 °C using 2.0 mol L^{-1} ethanol + 2 mol L^{-1} KOH

Shown in Fig. 4b are the forward curves from CV experiments, in order to make easier the observation of the details about these results.

As can be observed, PtAuIr/C 40:50:10 showed the highest catalytic activity toward ethanol electro-oxidation; using this material, the lowest onset potential (~−0.66 V) and the highest peak current density (50 mA per g of Pt) were obtained. It is important to point out that as the gold content in the materials increases, the catalytic activity increases. All the ternary electrocatalysts showed higher catalytic activity than Pt/C (peak current density ~ 14 mA per g of Pt). Au/C and Ir/C showed very low catalytic activity as already observed in the literature [3, 20]. The beneficial effect of gold in these ternary electrocatalysts which improves the catalytic activity toward ethanol electro-oxidation is evident. According to the literature, Au decreases the adsorption energy of poisoning intermediates on Pt sites [3, 37]. In a previous study considering PtAu/C binary electrocatalysts for ethanol electro-oxidation, we also found that the material with 50% of gold showed higher catalytic activity than the other materials with lower gold content [3].

The chronoamperometry curves for ethanol electro-oxidation reaction on Pt/C, Au/C, Ir/C, and PtAuIr/C at potential of −0.35 V for 30 min are shown in Fig. 5. These experiments were done at −0.35 V because it is in a region where the potential is higher than the onset potential, apparently around the middle of the curve [3, 6, 20]. Additionally, this potential corresponds to 0.5 V vs RHE which is a typical potential for fuel cell operation [39]. As can be seen, the current density measured at 30 min of the experiment using the PtAuIr/C 40:50:10 electrocatalyst was the highest one in this study. The current density on PtAuIr/C 40:50:10 is about 18 times higher than that obtained for the Pt/C electrocatalyst. It is important to stress that the current density obtained using PtAuIr/C 40:50:10 at the end of the CA experiment is about 30% higher than that reported previously using PtAu/C 50:50 [3]. Thus, iridium also contributes to the improvement of the catalytic activity of PtAu/C. In a previous publication, we have shown that iridium promotes an improvement in the catalytic activity of platinum toward ethanol electro-oxidation [20]. The improvement in the catalytic activity of platinum toward ethanol caused by iridium might be related to the OH_{ads} species formed at low overpotential on Ir and by the disturbance at platinum orbital by Ir atoms that might decrease the poisoning on the catalyst surface [4, 5, 20, 40]. Additionally, gold can extend the platinum lattice parameter by alloying, which is beneficial to the ethanol C−C bond cleavage [3, 37].

Figure 6 shows the polarization and power density curves obtained in a single DEFC using Pt/C, Au/C, Ir/C, and PtAuIr/C as anode electrocatalysts. The results from the DEFC experiments are summarized in Table 1.

From Fig. 6 and Table 1, it is possible to observe that the best performance of the DEFC was obtained using PtAuIr/C 60:30:10. This result is not in agreement with that obtained using CV and CA experiments, in which PtAuIr/C 40:50:10 was the best electrocatalyst. The disagreement of electrochemical experiments with DEFC results were also observed in other works [6, 41, 42]. It is important to point out that the

Table 1 Main results obtained using a direct ethanol fuel cell: open circuit potential (OCV) and maximum power density (MPD) at 75 °C

Electrocatalyst compositions	OCV/V	MPD/mW cm^{-2}
PtAuIr/C 40:50:10	0.64	7.10
PtAuIr/C 50:40:10	0.65	6.69
PtAuIr/C 60:30:10	0.71	7.58
PtAuIr/C 70:20:10	0.61	5.98
PtAuIr/C 80:10:10	0.68	5.57
Pt/C	0.52	3.08
Au/C	0.38	1.66
Ir/C	0.54	2.78

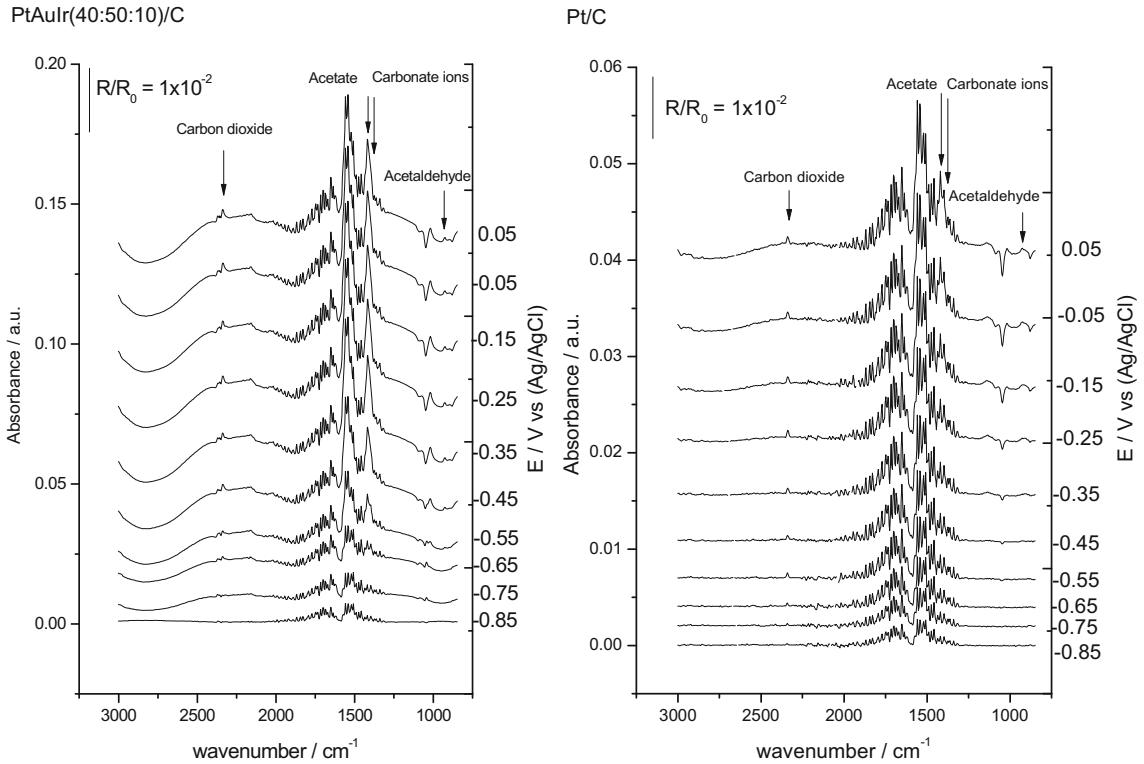

Fig. 7 In situ FTIR spectra taken at several potentials (indicated) in 1 mol L^{-1} KOH + 1.0 mol L^{-1} ethanol for electrocatalysts. The backgrounds were collected at −0.85 V

conditions of fuel cell experiments are quite different from conventional VC and CA electrochemical experiments, e.g., the diffusion of the fuel through the catalytic layer, the continuous and constant flux, and the temperature. Additionally, ethanol energy activation changes with the temperature; this change might result in a different interaction of ethanol molecule with the catalyst materials [6, 27]. However, as in CV and CA experiments, better results were obtained using ternary PtAuIr/C compositions than on monometallic Pt/C, Ir/C, and Au/C, showing the synergetic effect between Pt, Au, and Ir toward ethanol electro-oxidation. Furthermore, in fuel cell experiments, it was also observed that higher amounts of Au increase the ethanol electro-oxidation.

Figure 7 shows the spectra obtained by the ATR-FTIR in situ spectroscopy technique measured during ethanol electro-oxidation [4, 13, 41]. The bands related to the asymmetric stretching of carbon dioxide (~2343 cm^{-1}), the stretching of the CO bond of carbonate ion (~1376 cm^{-1}), the symmetric stretching of acetate (~1407 cm^{-1}), and the rocking of acetaldehyde (~928 cm^{-1}) were measured. The region between 1640 and 1750 cm^{-1} was attributed to the vibrations of different species including the interfacial water and carbonyl groups [4, 43].

Figure 8 shows the results of integrated bands deconvoluted using Lorentzian line forms [4, 41, 43, 44]. As can be observed in Fig. 8a, b, the intensity of CO_2 and carbonate is higher using PtAuIr/C 40:50:10 than using Pt/C as electrocatalyst. It is important to stress that the intensity of carbonate decreases in potentials higher than −0.35 V; this could be related to the extension of OH^- near the electrode surface [45]. Using PtAuIr/C, the intensity of acetate and acetaldehyde are also higher than on Pt/C (Fig. 8c, d); this suggests that the kinetic of the overall reaction on PtAuIr/C 40:50:10 was faster than on Pt/C.

In order to assess the comparative relation between the electrocatalysts, the integrated band intensity ratios of acetate/CO_2 are shown in Fig. 8e. The intensity of acetate/CO_2 is lower for PtAuIr/C 40:50:10 in the potential range from −0.75 to ~−0.25 V, indicating a preferential oxidation of ethanol to CO_2 (reaction proceeds toward 12 electron paths) [13, 46]. On the other hand, the intensity of acetate/CO_2 on Pt/C is higher indicating low selectivity to CO_2 as also observed in our previous publication [43]. It is important to point out that at high potentials (higher than ~−0.25 V) the intensity of acetate/CO_2 is higher on Pt/C which totally makes sense, because Pt/C is not able to oxidize CO at low potential; thus, all the CO blocking the Pt nanoparticle surface is oxidized to CO_2 at high potential. Furthermore, it is well known that the addition of Au and Ir to Pt promotes the CO electro-oxidation at lower potential than only Pt [47, 48].

Based on the ATR-FTIR results, it is possible to observe that the C−C cleavage is favored on PtAuIr/C 40:50:10.

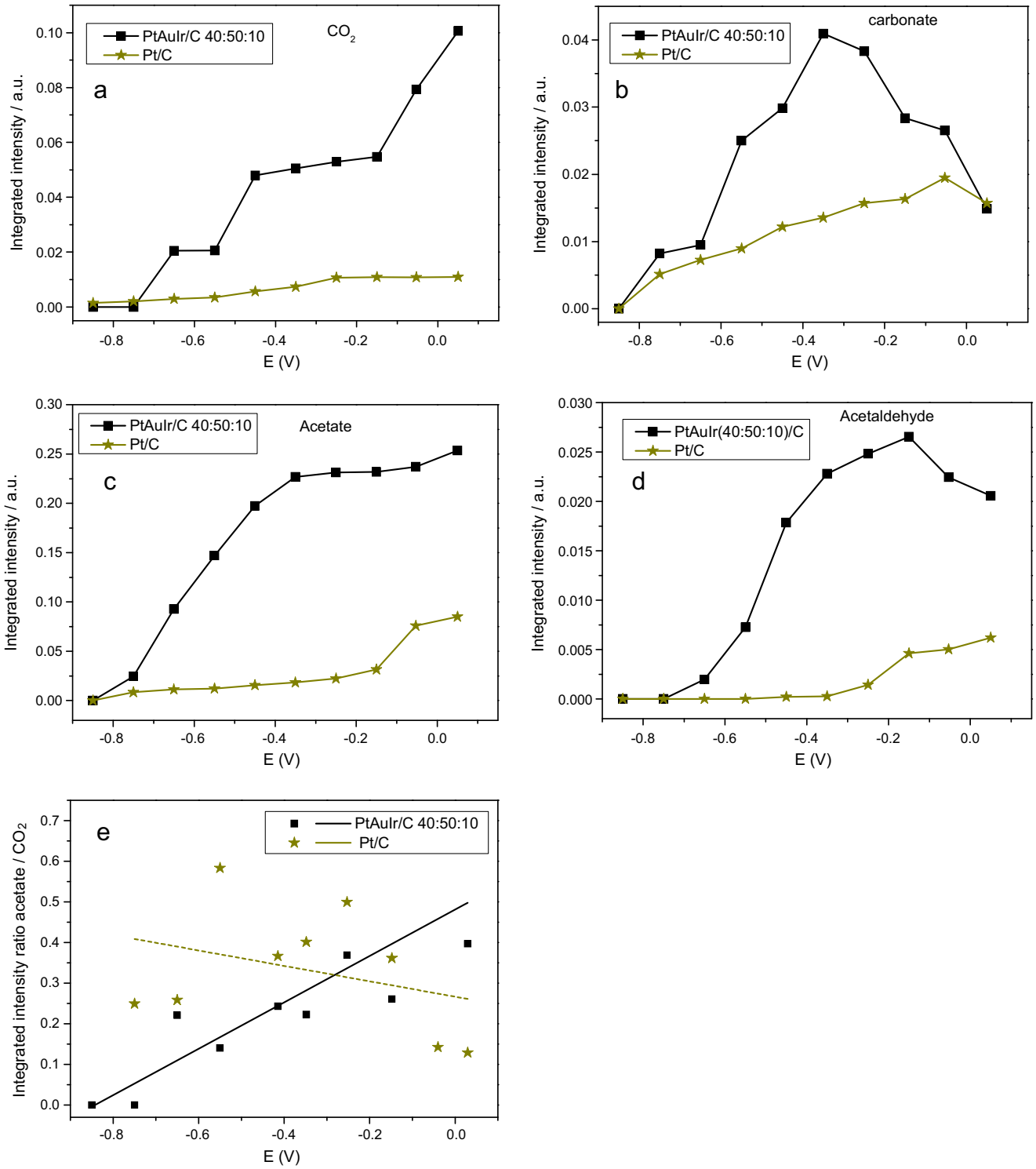

Fig. 8 Normalized intensities of carbon dioxide (**a**), carbonate (**b**), acetate (**c**), and acetaldehyde (**d**) as a function of the potential for the electrocatalysts. Band intensity ratios of acetate/carbon dioxide (**e**)

Conclusion

The results of this work show that Au and Ir improve the catalytic activity of Pt toward ethanol electro-oxidation as shown by electrochemical and fuel cell experiments. The XRD results suggest that PtAuIr alloy was formed. TEM analysis revealed that the particle sizes are from 2 to 11 nm for all PtAuIr/C electrocatalysts. PtAuIr/C 40:50:10 shows the best catalytic activity toward ethanol electro-oxidation in CV and CA experiments. The current density at the end of CA

experiments using PtAuIr/C 40:50:10 was 18 times higher than using Pt/C. However, the best fuel cell performance was obtained using PtAuIr/C 60:30:10 as anode. The improvement in the catalytic activity of platinum toward ethanol is attributed to Au that decreases the adsorption energy of poisoning intermediates on Pt sites and by Ir that provides OH_{ads} species at low overpotential and also promotes a disturbance at platinum orbital that might decrease the poisoning on the catalyst surface.

Acknowledgements The authors wish to thank CNPq (141469/2013-7), FAPESP (14/09087-4), FAPESP (14/50279-4), and Capes for the financial support, and also the Laboratório de Microscopia do Centro de Ciências e Tecnologia de Materiais (CCTM) for TEM measurements.

References

1. Sun C-L, Tang J-S, Brazeau N, Wu J-J, Ntais S, Yin C-W et al (2015) Particle size effects of sulfonated graphene supported Pt nanoparticles on ethanol electrooxidation. Electrochim Acta 162: 282–289
2. Kamarudin MZF, Kamarudin SK, Masdar MS, Daud WRW (2014) Review: Direct ethanol fuel cells. Int J Hydrog Energy 38(22): 9438–9453
3. da Silva SG, Silva JCM, Buzzo GS, De Souza RFB, Spinacé EV, Neto AO et al (2014) Electrochemical and fuel cell evaluation of PtAu/C electrocatalysts for ethanol electro-oxidation in alkaline media. Int J Hydrog Energy 39:10121–10127
4. Silva JCM, Anea B, De Souza RFB, Assumpcao MHMT, Calegaro ML, Neto AO et al (2013) Ethanol oxidation reaction on IrPtSn/C electrocatalysts with low Pt content. J Braz Chem Soc 24:1553–1560
5. Shen SY, Zhao TS, Xu JB (2010) Carbon-supported bimetallic PdIr catalysts for ethanol oxidation in alkaline media. Electrochim Acta 55:9179–9184
6. Neto AO, da Silva SG, Buzzo GS, de Souza RFB, Assumpção MHMT, Spinacé EV et al (2015) Ethanol electrooxidation on PdIr/C electrocatalysts in alkaline media: electrochemical and fuel cell studies. Ionics 21:487–495
7. González-Quijano D, Pech-Rodríguez WJ, Escalante-García JI, Vargas-Gutiérrez G, Rodríguez-Varela FJ (2014) Electrocatalysts for ethanol and ethylene glycol oxidation reactions. Part I: effects of the polyol synthesis conditions on the characteristics and catalytic activity of Pt–Sn/C anodes. Int J Hydrog Energy 39:16676–16685
8. Sieben JM, Duarte MME (2012) Methanol, ethanol and ethylene glycol electro-oxidation at Pt and Pt–Ru catalysts electrodeposited over oxidized carbon nanotubes. Int J Hydrog Energy 37:9941–9947
9. Shen SY, Zhao TS, Xu JB (2010) Carbon supported PtRh catalysts for ethanol oxidation in alkaline direct ethanol fuel cell. Int J Hydrog Energy 35:12911–12917
10. Beyhan S, Uosaki K, Feliu JM, Herrero E (2013) Electrochemical and in situ FTIR studies of ethanol adsorption and oxidation on gold single crystal electrodes in alkaline media. J Electroanal Chem 707: 89–94
11. Busó-Rogero C, Brimaud S, Solla-Gullon J, Vidal-Iglesias FJ, Herrero E, Behm RJ et al (2016) Ethanol oxidation on shape-controlled platinum nanoparticles at different pHs: a combined in situ IR spectroscopy and online mass spectrometry study. J Electroanal Chem 763:116–124
12. Chen Y, Shi J, Chen S (2015) Small-molecule (CO, H2) electro-oxidation as an electrochemical tool for characterization of Ni@Pt/C with different Pt coverages. J Phys Chem C 119:7138–7145
13. Silva JCM, Parreira LS, De Souza RFB, Calegaro ML, Spinacé EV, Neto AO et al (2011) PtSn/C alloyed and non-alloyed materials: differences in the ethanol electro-oxidation reaction pathways. Appl Catal B Environ 110:141–147
14. Zignani SC, Baglio V, Linares JJ, Monforte G, Gonzalez ER, Aricò AS (2012) Performance and selectivity of PtxSn/C electro-catalysts for ethanol oxidation prepared by reduction with different formic acid concentrations. Electrochim Acta 70:255–265
15. Tayal J, Rawat B, Basu S (2011) Bi-metallic and tri-metallic Pt-Sn/C, Pt-Ir/C, Pt-Ir-Sn/C catalysts for electro-oxidation of ethanol in direct ethanol fuel cell. Int J Hydrog Energy 36(22):14884–14897
16. Wang Z-B, Yin G-P, Lin Y-G (2007) Synthesis and characterization of PtRuMo/C nanoparticle electrocatalyst for direct ethanol fuel cell. J Power Sources 170:242–250
17. Ammam M, Easton EB (2012) Quaternary PtMnCuX/C (X = Fe, Co, Ni, and Sn) and PtMnMoX/C (X = Fe, Co, Ni, Cu and Sn) alloys catalysts: synthesis, characterization and activity towards ethanol electrooxidation. J Power Sources 215:188–198
18. Fatih K, Neburchilov V, Alzate V, Neagu R, Wang H (2010) Synthesis and characterization of quaternary PtRuIrSn/C electrocatalysts for direct ethanol fuel cells. J Power Sources 195: 7168–7175
19. Li H, Wu H, Zhai Y, Xu X, Jin Y (2013) Synthesis of monodisperse plasmonic Au core–Pt shell concave nanocubes with superior catalytic and electrocatalytic activity. ACS Catal 3:2045–2051
20. da Silva SG, Assumpção MHMT, de Souza RFB, Buzzo GS, Spinacé EV, Neto AO et al (2014) Electrochemical and fuel cell evaluation of PtIr/C electrocatalysts for ethanol electrooxidation in alkaline medium. Electrocatalysis 5:438–444
21. Tayal J, Rawat B, Basu S (2011) Bi-metallic and tri-metallic Pt–Sn/C, Pt–Ir/C, Pt–Ir–Sn/C catalysts for electro-oxidation of ethanol in direct ethanol fuel cell. Int J Hydrog Energy 36:14884–14897
22. Dutta A, Mahapatra SS, Datta J (2011) High performance PtPdAu nano-catalyst for ethanol oxidation in alkaline media for fuel cell applications. Int J Hydrog Energy 36:14898–14906
23. Wang X, Zhu F, He Y, Wang M, Zhang Z, Ma Z et al (2016) Highly active carbon supported ternary PdSnPtx (x = 0.1–0.7) catalysts for ethanol electro-oxidation in alkaline and acid media. J Colloid Interface Sci 468:200–210
24. Li M, Kowal A, Sasaki K, Marinkovic N, Su D, Korach E et al (2010) Ethanol oxidation on the ternary Pt-Rh-SnO2/C electrocatalysts with varied Pt:Rh:Sn ratios. Electrochim Acta 55: 4331–4338
25. Neto AO, Tusi MM, de Oliveira Polanco NS, da Silva SG, Coelho dos Santos M, Spinacé EV (2011) PdBi/C electrocatalysts for ethanol electro-oxidation in alkaline medium. Int J Hydrog Energy 36: 10522–10526
26. Assumpção MHMT, da Silva SG, de Souza RFB, Buzzo GS, Spinacé EV, Neto AO et al (2014) Direct ammonia fuel cell performance using PtIr/C as anode electrocatalysts. Int J Hydrog Energy 39:5148–5152
27. Hou H, Wang S, Jin W, Jiang Q, Sun L, Jiang L et al (2011) KOH modified Nafion112 membrane for high performance alkaline direct ethanol fuel cell. Int J Hydrog Energy 36:5104–5109
28. Assumpção MHMT, Piasentin RM, Hammer P, De Souza RFB, Buzzo GS, Santos MC et al (2015) Oxidation of ammonia using PtRh/C electrocatalysts: fuel cell and electrochemical evaluation. Appl Catal B Environ 174–175:136–144
29. Assumpção MHMT, da Silva SG, De Souza RFB, Buzzo GS, Spinacé EV, Santos MC et al (2014) Investigation of PdIr/C electrocatalysts as anode on the performance of direct ammonia fuel cell. J Power Sources 268:129–136

30. De Souza RFB, Silva JCM, Simoes FC, Calegaro ML, Neto AO, Santos MC (2012) New approaches for the ethanol oxidation reaction of Pt/C on carbon cloth using ATR-FTIR. Int J Electrochem Sci 7:5356–5366
31. Henrique RS, De Souza RFB, Silva JCM, Ayoub JMS, Piasentin RM, Linardi M et al (2012) Preparation of Pt/C-In2O3 center dot SnO2 electrocatalysts by borohydride reduction process for ethanol electro-oxidation. Int J Electrochem Sci 7:2036–2046
32. Lee AF, Baddeley CJ, Hardacre C, Ormerod RM, Lambert RM, Schmid G et al (1995) Structural and catalytic properties of novel Au/Pd bimetallic colloid particles: EXAFS, XRD, and acetylene coupling. J Phys Chem 99:6096–6102
33. Geraldes AN, da Silva DF, Pino ES, da Silva JCM, de Souza RFB, Hammer P et al (2013) Ethanol electro-oxidation in an alkaline medium using Pd/C, Au/C and PdAu/C electrocatalysts prepared by electron beam irradiation. Electrochim Acta 111:455–465
34. Silva JCM, da Silva SG, De Souza RFB, Buzzo GS, Spinacé EV, Neto AO et al (2015) PtAu/C electrocatalysts as anodes for direct ammonia fuel cell. Appl Catal A Gen 490:133–138
35. Neto AO, da Silva SG, Buzzo GS, de Souza RFB, Assumpção MHMT, Spinacé EV et al (2014) Ethanol electrooxidation on PdIr/C electrocatalysts in alkaline media: electrochemical and fuel cell studies. Ionics:1–9
36. Kamarudin MZF, Kamarudin SK, Masdar MS, Daud WRW (2013) Review: direct ethanol fuel cells. Int J Hydrog Energy 38:9438–9453
37. Zhou W, Li M, Zhang L, Chan SH (2014) Supported PtAu catalysts with different nano-structures for ethanol electrooxidation. Electrochim Acta 123:233–239
38. Jiang L, Hsu A, Chu D, Chen R (2010) Ethanol electro-oxidation on Pt/C and PtSn/C catalysts in alkaline and acid solutions. Int J Hydrog Energy 35:365–372
39. Rizo R, Sebastián D, Lázaro MJ, Pastor E (2017) On the design of Pt-Sn efficient catalyst for carbon monoxide and ethanol oxidation in acid and alkaline media. Appl Catal B Environ 200:246–254
40. Ribeiro J, dos Anjos DM, Kokoh KB, Coutanceau C, Léger JM, Olivi P et al (2007) Carbon-supported ternary PtSnIr catalysts for direct ethanol fuel cell. Electrochim Acta 52:6997–7006
41. De Souza RFB, Parreira LS, Silva JCM, Simões FC, Calegaro ML, Giz MJ et al (2011) PtSnCe/C electrocatalysts for ethanol oxidation: DEFC and FTIR "in-situ" studies. Int J Hydrog Energy 36:11519–11527
42. Li G, Jiang L, Jiang Q, Wang S, Sun G (2011) Preparation and characterization of PdxAgy/C electrocatalysts for ethanol electrooxidation reaction in alkaline media. Electrochim Acta 56:7703–7711
43. Fontes EH, Piasentin RM, Ayoub JMS, da Silva JCM, Assumpção MHMT, Spinacé EV et al (2015) Electrochemical and in situ ATR-FTIR studies of ethanol electro-oxidation in alkaline medium using PtRh/C electrocatalysts. Materials for Renewable and Sustainable Energy 4:3
44. Neto AO, Nandenha J, Assumpção MHMT, Linardi M, Spinacé EV, de Souza RFB (2013) In situ spectroscopy studies of ethanol oxidation reaction using a single fuel cell/ATR-FTIR setup. Int J Hydrog Energy 38:10585–10591
45. Figueiredo MC, Arán-Ais RM, Climent V, Kallio T, Feliu JM (2015) Evidence of local pH changes during ethanol oxidation at Pt electrodes in alkaline media. ChemElectroChem 2:1254–1258
46. Lima FHB, Gonzalez ER (2008) Ethanol electro-oxidation on carbon-supported Pt-Ru. Pt-Rh and Pt-Ru-Rh nanoparticles Electrochimica Acta 53:2963–2971
47. Feng J-J, He L-L, Fang R, Wang Q-L, Yuan J, Wang A-J (2016) Bimetallic PtAu superlattice arrays: highly electroactive and durable catalyst for oxygen reduction and methanol oxidation reactions. J Power Sources 330:140–148
48. Chen D, Chen R, Dang D, Shu T, Peng H, Liao S (2014) High performance of core–shell structured Ir@Pt/C catalyst prepared by a facile pulse electrochemical deposition. Electrochem Commun 46:115–119